The linker histone H1.2 is a novel component of the nucleolar organizer regions

Junjie Chen, Boon Heng Dennis Teo, Yitian Cai, Seng Yin Kelly Wee, and Jinhua Lu[1]

From the Department of Microbiology and Immunology, Yong Loo Lin School of Medicine and Immunology Programme, National University of Singapore, Singapore 117697

Edited by Joel Gottesfeld

The nucleoli accumulate rRNA genes and are the sites of rRNA synthesis and rRNA assembly into ribosomes. During mitosis, nucleoli dissociate, but nucleolar remnants remain on the rRNA gene loci, forming distinct nucleolar organizer regions (NORs). Little is known about the composition and structure of NORs, but upstream binding factor (UBF) has been established as its master organizer. In this study, we sought to establish new proteins in NORs. Using UBF-Sepharose to isolate UBF-binding proteins, we identified histone H1.2 as a candidate partner but were puzzled by this observation, given that UBF is known to be located predominantly in nucleoli, whereas H1.2 distributed broadly among the chromatins in interphase nuclei. We then examined cells undergoing mitosis and saw that both H1.2 and UBF were recruited into NORs in this state, reconciling the results of our UBF pulldowns. Inhibiting rRNA synthesis in interphase nuclei also induced NOR-like structures containing both UBF and H1.2. When chromosomes were isolated and spread on coverslips, NORs appeared separated from the chromosomes containing both UBF and H1.2. After chromosomes were fragmented by homogenization, intact NORs remained visible. Results collectively suggest that NORs are independent structures and that the linker histone H1.2 is a novel component of this structure.

Nucleoli are distinct nuclear bodies in which rRNA genes (rDNA)[2] are congregated and rRNA is synthesized and assembled into ribosomes (1–3). At interphase, nucleoli occupy significant nuclear domains around the rDNA loci. At mitosis, nucleoli disintegrate but remnants remain on rDNA, forming the nucleolar organizer regions (NORs) (4, 5). The structure of interphase nucleoli was proposed largely based on transmission electron micrographs with an overall tripartite organization (3, 6). However, the composition and structure of NORs remain poorly delineated (7).

Based on the tripartite model, an interphase nucleolus is composed of one or more fibrillar centers (FCs) each being surrounded by a dense fibrillar component (DFC), and these FC/DFC units are embedded in a greater granular component (GC) (8–10). These nucleoli are encircled by a dense layer of perinucleolar heterochromatins, but chromatins are otherwise scarce in the nucleolar lumen (11, 12). In live cells, nucleolar proteins can be highly dynamic and mobile (13). In fact, liquid-like properties have been ascribed to nucleoli and other nuclear domains (14, 15). Nonetheless, nucleoli still display substantial structural independence and can be isolated from homogenized nuclei (12, 16, 17). The structural independence of NORs has not been assessed.

The tripartite nucleolar structural model aligns well with the known function of nucleoli in ribosome generation. rDNA and elements of the rRNA transcription machinery are located in the innermost FC regions (3, 10). rRNA transcription takes place at the FC/DFC interface where newly synthesized pre-rRNA accumulates (18, 19). Each rRNA gene can be simultaneously transcribed in tandem by multiple RNA polymerase (Pol) I, giving rise to tandem rRNA transcripts that stem from each rDNA locus like a "Christmas tree" (20, 21). rRNA is processed in the DFC region and incorporated into ribosomes in the GC region (3, 10).

During mitosis when rRNA transcription arrests, nucleoli disintegrate, but nucleolar remnants remain associated with the rDNA loci to form NORs (7, 22). Some elements of the nucleolar FC domains are recruited into NORs, but GC and DFC elements disperse at this stage (23, 24). Like the chromatids, NORs also divide equivalently into daughter nuclei and then re-emerge as nucleoli (22). The rDNA loci reside on acrocentric chromosomes, and NORs form adjacent to these rDNA loci, which, unlike the rest of the chromosomal regions, assume distinctly open configurations (25, 26). These nucleolar remnants precipitate silver nitrite and are therefore also known as AgNORs (27). The detailed NOR structure and composition, however, are not understood, and the rDNA loci remain incompletely sequenced (7).

Upstream binding factor (UBF), a Pol I-associated transcription factor, is a nucleolar protein that appears essential to both NOR and nucleolus formation around the rDNA loci. Each active rRNA gene contains a core promoter, which is recognized by selective factor 1, and it also contains an upstream enhancer element that is bound by UBF. These jointly recruit
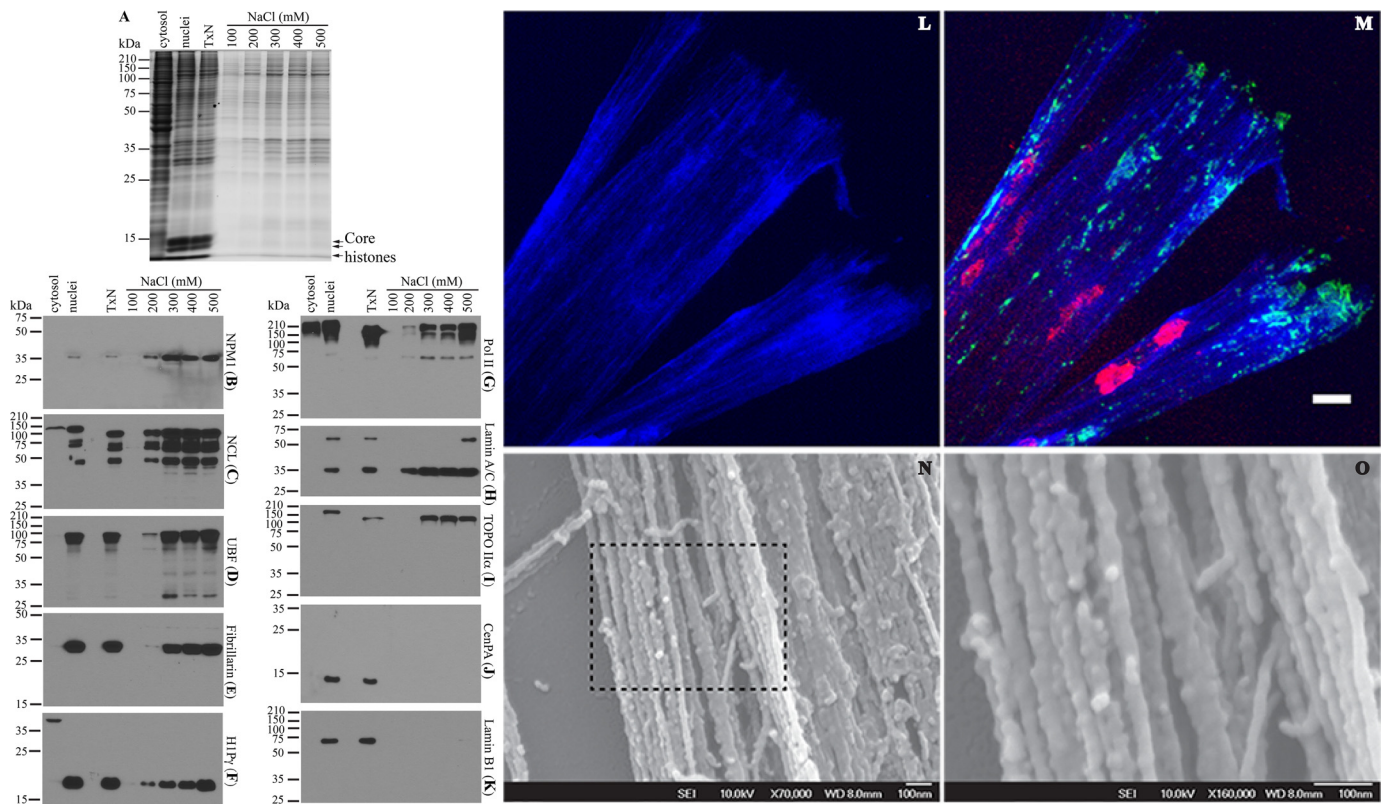
Figure 1. Extraction of nuclear proteins from the chromatins. *A*, TxN in the 0.25 M sucrose buffer were made 100–500 mM with NaCl. After vigorously pipetting and centrifugation, supernatants were analyzed by SDS-PAGE Coomassie Blue staining. Cytosol, isolated nuclei, and TxN were also included. *B–K*, cytosol, nuclei, TxN, and the nuclear extracts were probed by Western blotting with mouse and rabbit antibodies specific for nucleolar (NPM1, fibrillarin, nucleolin (*NCL*), and UBF), nuclear lamina (lamins A, C, and B1), and some chromatin-associated (centromere protein A (*CenPA*), HP1γ, RNA pol II, and TopoIIα) proteins. Horseradish peroxidase–conjugated goat anti-mouse and anti-rabbit IgG were used as secondary antibodies. *L* and *M*, TxN on coverslips were exposed to 500 mM NaCl for 15 min, fixed, and stained for lamin B1 (AF488, *green*), NPM1 (Cy3, *red*), and chromatin (4,6-diamino-2-phenylindole (DAPI), *blue*). *L*, chromatins. *M*, merged signals. *Scale bar*, 5 μm. *N* and *O*, NaCl-extracted TxN on coverslips were processed for SEM analysis. Images were shown at two different magnifications: *N*, ×70,000. *O*, ×160,000. The *square* in *N* is equivalent to the image in *O*.

Pol I to initiate rRNA transcription (28). In *Xenopus*, UBF binds not only to the rDNA enhancer but also broadly to other sites in the rDNA locus (29, 30). Ectopic introduction of these tandemly engineered *Xenopus* UBF-binding elements into human HT1080 cells demonstrated recruitment of human UBF and Pol I transcription elements to form pseudo-NORs at mitosis and induce nucleolar FC-like structures at interphase (31). When the ectopic DNA construct was completed with rRNA-coding sequences, these engineered neo-rDNA loci were able to develop into nucleoli in interphase nuclei, producing rRNA and ribosomes (32). This demonstrates the instrumental roles of UBF in the structure and functions of NORs and the nucleoli.

We argued that by identifying new UBF-binding proteins in the nuclei, novel insights could be obtained into the structure and functions of the nucleoli and NORs. Using UBF-Sepharose, we have identified the linker histone H1.2 as a prominent UBF-binding protein, and it was shown to follow UBF into NORs. These NORs containing UBF and H1.2 were structurally separable from chromosomes.

Results

Generation of nuclear extract

To identify UBF-binding proteins, we first prepared a soluble extract from isolated nuclei. Nuclei rather than nucleoli were used because UBF also binds to selected genes outside the

nucleoli and regulates RNA Pol II-mediated gene expression (33–35). The nuclei were first extracted with Triton X-100 to deplete the nuclear envelope, and these nuclei, known as TxN, mostly remained intact and oval and retained the nuclear protein profile (data not shown; Fig. 1*A*). Proteins were then test-extracted from TxN at increasing NaCl concentrations (100–500 mM). Protein extraction plateaued at 400–500 mM NaCl (Fig. 1*A*). The otherwise particulate TxN burst into one colloidal gel at 500 mM NaCl (data not shown), suggestive of dissociation of the nuclear scaffold from the chromatins. The nuclear extracts lacked significant core histones, which ruled out significant chromatin contamination (Fig. 1*A*). For affinity pull-downs, nuclear extract was routinely extracted from TxN at 500 mM NaCl, known as TxNE. Briefly, nuclei were isolated after centrifugation through 2.2 M sucrose and extracted with Triton X-100 to generate TxN (Fig. 1*A*). TxNE is obtained by extracting TxN at 500 mM NaCl.

The inclusiveness of TxNE as a nuclear extract was surveyed by detecting representative nucleolar and nuclear proteins (Fig. 1, *B–K*). The nucleolar proteins NPM1 (nucleophosmin-1), nucleolin, UBF and fibrillarin were all detectable from the 300 mM NaCl extract (Fig. 1, *B–E*). The intimately chromatin-associated proteins HP1γ (heterochromatin protein 1γ), Pol II, lamin A/C, and topoisomerase IIα (TopoIIα) were also extracted (Fig. 1, *F–I*). In contrast, centromere protein A and the
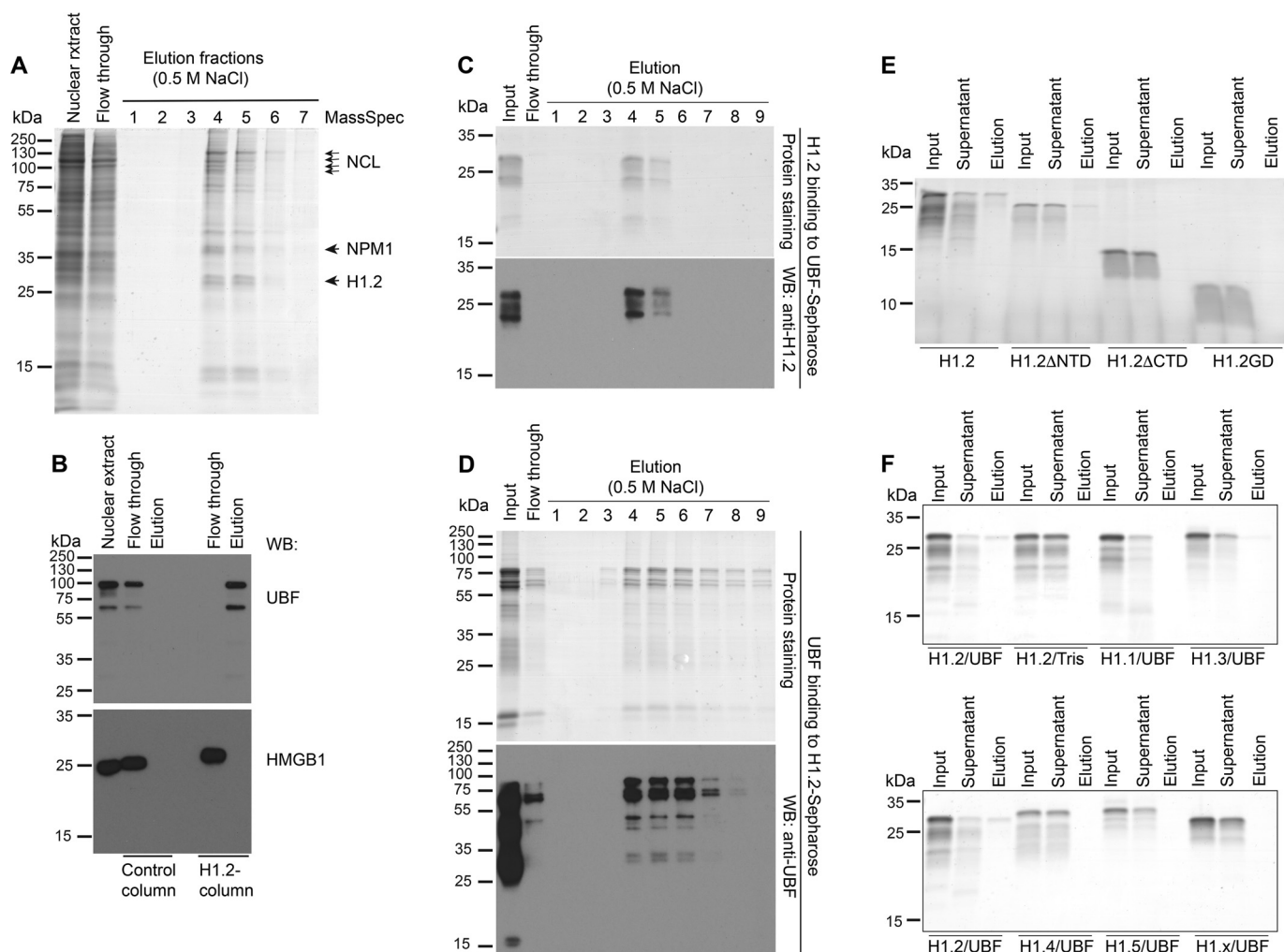
Figure 2. Histone H1.2 is a novel UBF-binding protein. *A*, TxNE (1 ml) was 1:1 diluted with 50 mM Tris (pH 7.4) and incubated with UBF-Sepharose (0.5 ml) for 2 h at 4 °C in a column. The column was washed and eluted at 500 mM NaCl. The first seven fractions, the input TxNE, and the flowthrough were analyzed by SDS-PAGE and Coomassie Blue staining. *B*, diluted TxNE (2 ml) was incubated with 0.5 ml of H1.2-Sepharose and, as a control, Tris-Sepharose. After elution, fractions 4–6 were combined (elution). The input TxNE, the flowthrough fraction, and the elution were analyzed by Western blotting using anti-UBF and anti-HMGB1 antibodies. *C*, recombinant H1.2 (2 ml) was incubated with UBF-Sepharose, and the bound proteins were eluted. Input H1.2, the flowthrough, and eluted fractions were analyzed by SDA-PAGE Coomassie Blue staining (*upper panel*) and Western blotting (*lower panel*). *D*, recombinant UBF (2 ml) was incubated with H1.2-Sepharose. The input UBF, the flowthrough, and eluted fractions were analyzed by SDS-PAGE (*upper panel*) and Western blotting (*lower panel*). *E*, the three purified H1.2 mutants H1.2ΔNTD, H1.2ΔCTD, and H1.2GD (200 μl) were each incubated with 50 μl of UBF-Sepharose for 2 h. Protein input, the absorbed supernatants, and the elution were compared by SDS-PAGE Coomassie Blue staining. Samples were examined on 18% (w/v) gels. *F*, purified H1.1, H1.2, H1.3, H1.4, H1.5, and H1.x were similarly incubated with UBF-Sepharose. As a negative control, H1.2 was incubated with Tris-Sepharose (Tris). The input proteins, absorbed supernatants, and elution were compared on 12.5% (w/v) gels.

nuclear lamina protein LB1 (lamin B1) were absent (Fig. 1, *J* and *K*). Overall, TxNE is highly inclusive of nuclear proteins without significant chromatin contamination.

To view changes in nuclear chromatin organization upon NaCl extraction, TxN were first adhered to coverslips and then exposed to 100–500 mM of NaCl. TxN became increasingly swollen at rising NaCl concentrations (data not shown). At 500 mM NaCl, TxN burst into extended and often parallel chromatin fibers (Fig. 1*L*). The otherwise continuous nuclear lamina, as identified by LB1, fractured and scattered among the chromatin fibers (Fig. 1*M*). By scanning electron microscopy (SEM), the burst TxN displayed parallel fibers corresponding to chromatins (Fig. 1, *N* and *O*).

Histone H1.2 is a novel UBF-binding protein

UBF-Sepharose was prepared from recombinant UBF and used in affinity chromatography with TxNE. Proteins were eluted from UBF-Sepharose using 500 mM NaCl, which showed heterogeneity in size (Fig. 2*A*). By LC-MS/MS (Table S1), a group of four high molecular weight proteins were all identified as nucleolin (Fig. 2*A*). A 36-kDa band was identified as NPM1. A 28-kDa region was abundant with a H1 histone variant H1.2 (Fig. 2*A*). Being nucleolar proteins, association of nucleolin and NPM1 to UBF-Sepharose was not surprising. However, H1.2 was not known to bind to UBF or to localize to the nucleoli.

H1.2–UBF interaction was further examined using H1.2-Sepharose and, as a control, Tris-Sepharose. After TxNE was applied on Tris-Sepharose, UBF remained abundant in the flowthrough fraction and was not subsequently eluted from the resins (Fig. 2*B*). With H1.2-Sepharose, UBF was depleted in the flowthrough fraction and subsequently eluted from the resins, suggesting UBF binding to H1.2. HMGB1 (high mobility group box 1) is structurally similar to UBF (36), but it showed
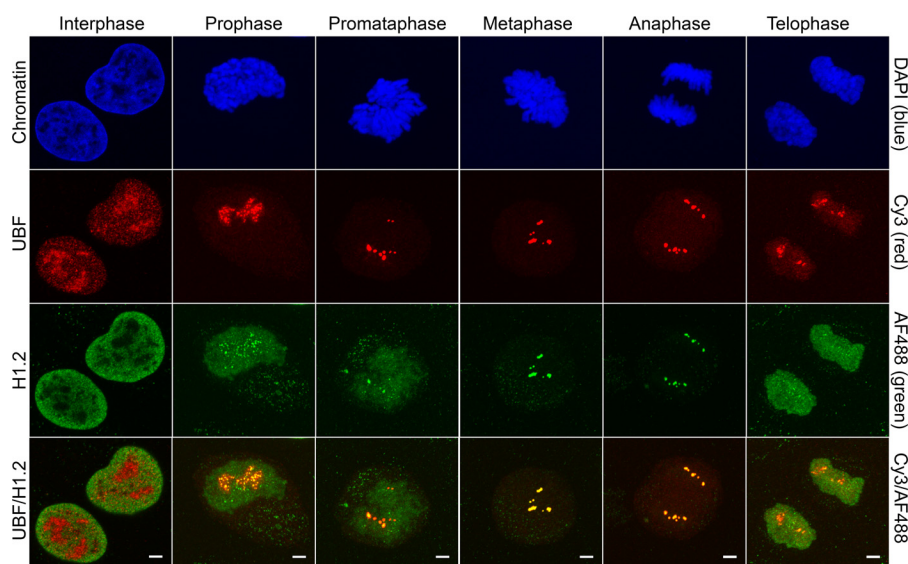
Figure 3. Cellular distribution of UBF and histone H1.2 in interphase and mitotic cells. HeLa cells were fixed, permeabilized, and incubated first with mouse anti-UBF and rabbit anti-H1.2 antibodies and then with secondary goat anti-mouse (Cy3, *red*) and anti-rabbit (Alexa Fluor 488 or AF488, *green*) IgG. The cells were mounted with a DAPI-containing medium and analyzed by confocal microscopy. The images were captured as 0.36-μm serial sections. Using the Imaris software, 3D images were reconstructed for the mitotic images. *Scale bars*, 5 μm.

no binding to Tris- or H1.2-Sepharose (Fig. 2*B*). This shows specific H1.2 binding to UBF.

Whether H1.2 interacts directly with UBF was evaluated with recombinant H1.2 and UBF proteins. When purified H1.2 was applied on UBF-Sepharose, it was completely depleted in the flowthrough fraction and was subsequently eluted from the resins, showing direct H1.2–UBF interaction (Fig. 2*C*). Likewise, purified UBF also bound to H1.2-Sepharose (Fig. 2*D*). This H1.2–UBF interaction was apparently disrupted at 500 mM NaCl, a condition at which bound UBF and H1.2 were eluted from the resins and TxNE was also eluted from the chromatins network (Fig. 1).

H1.2 contains three clearly demarcated domains: a central globular domain (GD) of ~80 amino acid residues, a short N-terminal domain (NTD), and a long C-terminal domain (CTD) of ~100 residues. We then examined which of the three H1.2 domains bound to UBF. To this end, these H1.2 mutants were generated by deleting its NTD, CTD, or both. As shown in Fig. 2*E*, after the short NTD was deleted, H1.2 still bound to UBF, but binding to UBF was abolished when CTD was deleted from H1.2. The H1.2 GD alone showed no binding to UBF. These results suggest that H1.2 binds to UBF through its CTD, which is more diversified than GD among the H1 variants (37). It is known that H1 binds to nucleosomes through the GD, whereas the H1 CTD binds more permissively to linker DNA, RNA, and potentially protein partners (38).

Disparate UBF and H1.2 distribution in interphase nuclei but co-localization at mitosis

Chromatins are abundant in the nucleoplasm but scarce in the nucleoli, and it is counterintuitive that H1.2, being a known chromatin-binding protein, also binds to UBF, which is a nucleolar protein (11). Staining of UBF and H1.2 in HeLa cells indeed revealed broad H1.2 distribution in the nucleoplasm, but UBF was concentrated in the chromatin-poor nucleoli (Fig. 3). UBF detection in the nucleoplasm was sparse overall (Fig. 3). Based on this largely disparate H1.2 and UBF distribution patterns, UBF-H1.2 interaction can only be expected at limited, if any, nucleoplasmic foci.

Examining mitotic cells, however, revealed condensation of both H1.2 and UBF in a number of granular NORs (Fig. 3). At sequential stages of mitosis, UBF and H1.2 exhibited distinct kinetics in NOR recruitments. At prometaphase, when all nuclear UBF apparently condensed in nine early NOR granules, only a fraction of H1.2 was found in these mitotic structures. Subsequently at metaphase, however, H1.2 was only detectable in NORs (Fig. 3).

During anaphase, NORs appeared to divide equivalently like the chromatids based on the intensity of UBF in the divided NORs (Fig. 3), as previously reported (22). H1.2 was also equivalently divided. At telophase, the chromatins began to unwind, and UBF also began to reorganize into nucleoli. H1.2 rapidly exited the nucleolar regions and became detectable among the unwinding chromatin network (Fig. 3). Mitotic cells develop NORs that contain different amounts of UBF. H1.2 appears to be recruited into these NORs in proportion with UBF. Because UBF is a housekeeping protein in NORs (31, 32), H1.2 could be recruited through its interaction with UBF.

H1.2 recruitment to NORs is a selective event

To gauge whether other nuclear proteins in addition to H1.2 are also recruited into mitotic NORs, mitotic cells were stained with a list of antibodies including those used in the Western blotting experiment shown in Fig. 1*A*, but none stained the NORs. For example, NPM1 and fibrillarin both localized to interphase nucleoli, but they dispersed from NORs during mitosis instead of being condensed into these structures (Fig. 4; data not shown). The human H1 histone family consists of 11 independently coded variants among which six (H1.1–H1.5 and H1.x) are somatically expressed (Fig. S1) (37). When H1.1, H1.3, H1.4, H1.5, and H1.x were immunostained, none were detected in NORs (Fig. S2), further demonstrating that H1.2
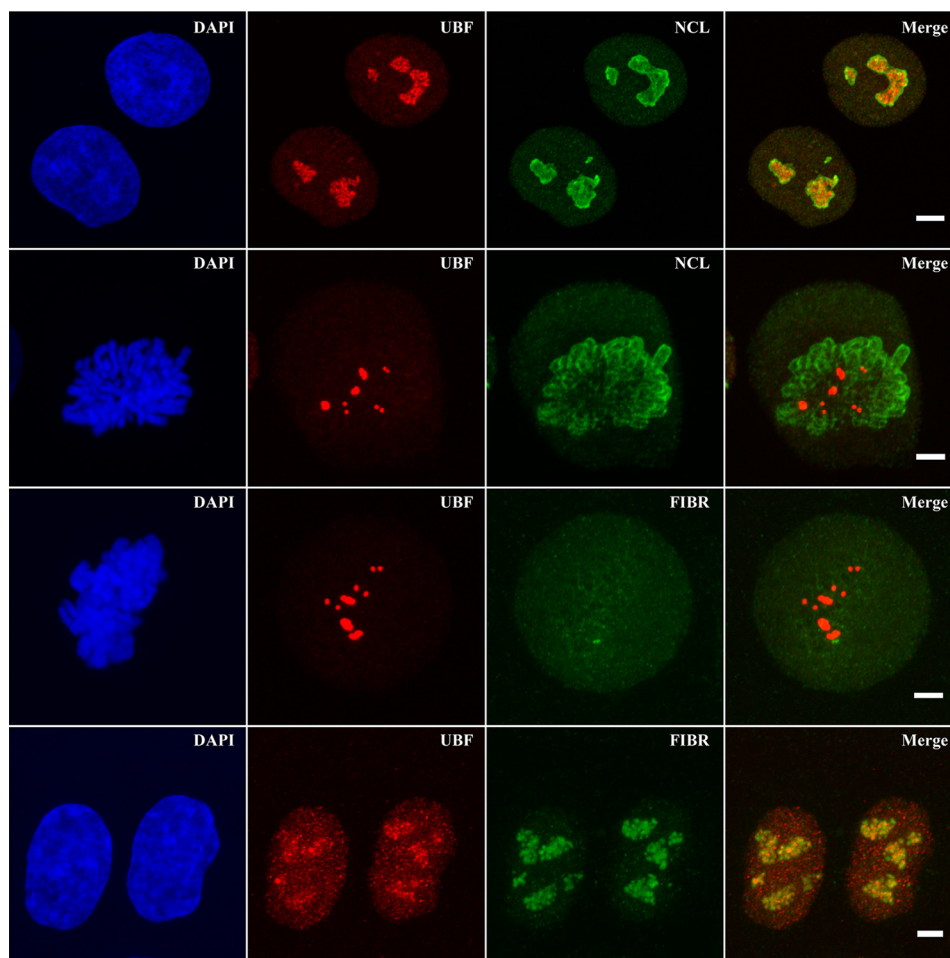
Figure 4. Dispersion of nucleolin and fibrillarin from mitotic NORs. Cells on coverslips were stained with mouse anti-UBF and rabbit anti-nucleolin (*NCL*) or anti-fibrillarin (*FIBR*) antibodies, followed by secondary goat anti-mouse (Cy3, *red*) and anti-rabbit IgG (AF488, *green*). After mounting using a DAPI-containing medium, interphase and prophase cell images were captured by confocal microscopy in 0.36-μm serial sections. 3D images were reconstructed using the Imaris software. Single and merged images are presented. *Scale bars*, 5 μm.

recruitment into NORs is a selective event. Interestingly, H1.x was concentrated in the interphase nucleoli (Fig. S2). This was also observed in a previous study (39). However, it dispersed at mitosis like fibrillarin (Fig. 4). H1.0 and H1.4 were also significantly detected outside the nuclei.

To examine whether other H1 variants also interact with UBF, recombinant H1.1, H1.3, H1.4, H1.5, and H1.x were similarly generated. In a pulldown study with UBF-Sepharose, these purified H1 variants were incubated for 2 h with UBF-Sepharose resins, which were then washed and eluted at 1 M NaCl. H1.2 was markedly depleted in the supernatant and subsequently eluted from the resin (Fig. 2F). As a control, it was not eluted from Tris-Sepharose. Among the other purified H1 variants, only H1.3 was eluted from the UBF-Sepharose resins (Fig. 2F). H1.1, H1.4, H1.5, and H1.x were not detectable in the elution. H1.3 is more closely related to H1.2 than the other H1 variants (Fig. S1). However, its expression in HeLa cells is too low to draw conclusions (Fig. S2).

Pol I inhibition causes UBF and H1.2 recruitment into NOR-like structures in interphase nuclei

In interphase cells, NOR-like granules can also be induced when Pol I is inhibited with low concentrations of actinomycin

D (ActD) (40, 41). When HeLa cells were treated for 2 h with ActD (40 ng/ml), UBF was shown to condense into NOR-like granules of different sizes (Fig. 5). H1.2 was proportionally recruited into all these structures, mirroring UBF and H1.2 recruitment into mitotic NORs (Fig. 3). It was also noted that only a fraction of total nuclear H1.2 and UBF condensed in the ActD-induced NORs, with the rest of each protein being broadly distributed among nucleoplasmic chromatins (Fig. 5). These two distinct pools of UBF and H1.2 may vary in the extents of their chromatin and other nuclear associations.

The nucleolar protein nucleolin was similarly stained in ActD-treated cells. Instead of being condensed into NORs, it dispersed from its original nucleolar locations and distributed broadly in the nuclei (Fig. 5). This shows that H1.2 recruitment to the UBF-demarcated NOR-like structures is selective for a distinct pool of H1.2. In both mitotic and ActD-induced recruitments, the arrest of rRNA transcription appeared to be a shared cause.

The cellular H1.2 levels were similar at interphase and metaphase

The detection of two pools of H1.2 in the ActD-treated interphase nuclei raised different interpretations with respect to the
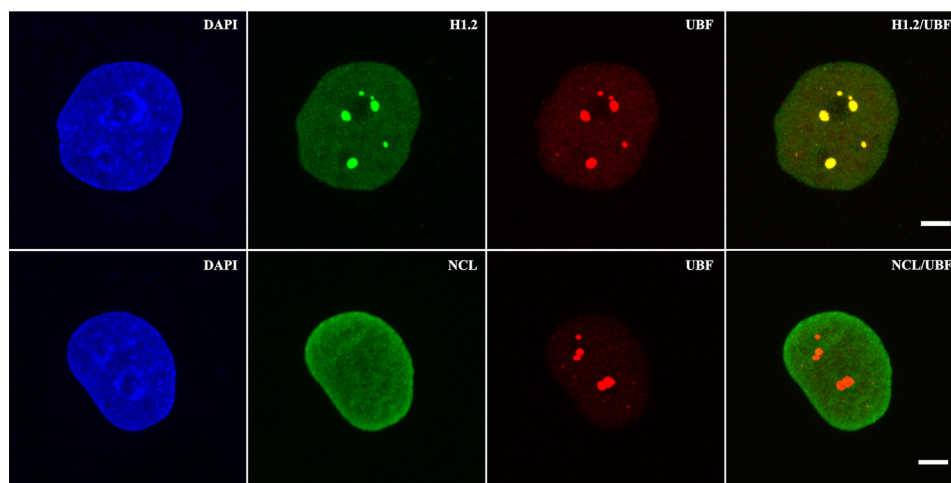
Figure 5. Inhibition of rRNA transcription in interphase nuclei causes H1.2 condensation into NOR-like structures. Cells cultured on coverslips were treated with ActD (40 ng/ml) for 2 h and then fixed, permeabilized, and stained using mouse anti-UBF and rabbit anti-H1.2 or anti-nucleolin (*NCL*) antibodies. The cells were then stained with secondary goat anti-mouse (Cy3, *red*) and anti-rabbit (AF488, *green*) IgG. After mounting with a DAPI-containing medium, the cells were analyzed by confocal microscopy capturing 0.36-μm serial sections. 3D images were reconstructed with single and merged signals. *Scale bars*, 5 μm.

NOR-associated H1.2: 1) most chromatin-associated H1.2 was degraded in mitotic cells, and therefore the NOR-associated H1.2 only represented a fraction of total H1.2; and 2) all cellular H1.2 was recruited into NORs. Considering the key roles of H1 histone in general chromatin compaction, neither of these are strong possibilities (42). Nonetheless, we measured total cellular H1.2 following colcemid-induced enrichment of metaphase cells. In these cultures, most HeLa cells are synchronized to metaphase after 15 h. The cells were treated with colcemid for up to 24 h but harvested at 3-h intervals. Total cellular H1.2 was determined by Western blotting, using UBF, TopoIIα, and LB1 as controls.

Total cellular UBF level showed steady increase from 9 h and appeared to plateau by 15 h (Fig. 6A). After 24 h, colcemid was removed from the culture, and within 6 h, total cellular UBF decreased to the basal level, and UBF fragments were noticed (Fig. 6A). The cellular level of TopoIIα, which is a major scaffold protein in chromatin compaction into chromosomes (43), largely mirrored that of UBF (Fig. 6A). In contrast, the total cellular levels of H1.2 and LB1 appeared unchanged throughout the colcemid treatment. This ruled out significant H1.2 degradation during mitosis (Fig. 6A), suggesting that either all cellular H1.2 followed UBF into NORs at mitosis or, as a third possibility, the chromatin-associated H1.2 is shielded from antibody detection in the compact chromosomes.

NORs are separable from chromosomes

UBF and the rDNA loci are perceived to be the backbones of NORs (31, 32). The extent of NOR structural independence relative to the chromosomes remain unclear. With the colcemid-induced metaphase cells, we examined the physical relationship between NORs and the chromosomes by isolating chromosome assemblies from these cells.

Unlike interphase chromatins, the chromosomes are fragile during homogenization. However, many intact chromosome assemblies could be generated with mild homogenization at 18-μm clearance. Some chromosome assemblies spread apart on coverslips, revealing significant gaps among chromosomes

and also physical relationships between NORs and the chromosomes (Fig. 6B). NORs remained intact but showed clear separation from the chromosomes, containing both UBF and H1.2 (Fig. 6, C and 6D). They appeared loosely tethered to, rather than being integral parts of, the chromosomes (Fig. 6, E and F). H1.2 remained in complete co-localization with UBF in these NORs (Fig. 6G). An additional observation from these spread chromosomes was the presence of H1.2 inside the chromosomes as well as the NORs (Fig. 6, C and F), in contrast to the lack of H1.2 detection in endogenous chromosomes (Fig. 3).

Endogenous chromosomes contain compacted H1.2

To examine the possibility that endogenous chromosomes compact H1.2 from antibody detection, the cells were treated with DNase after fixation and permeabilization. As shown in Fig. 7, a 30-min DNase treatment of the cells diminished chromatins in the endogenous chromosomes, but NORs remained intact containing both UBF and H1.2. Interestingly, H1.2 also became detectable among the residual chromosomes. Because NORs were still intact and abundant with H1.2, the newly revealed chromosomal H1.2 must have been otherwise compacted by chromatins from antibody detection.

NORs can be detached from chromosomes

We also homogenized the colcemid-enriched metaphase cells under more stringent conditions (10 μm clearance) that fragmented most chromosomes (Fig. 8A). In these homogenates, many particles were stained positive for UBF (Fig. 8B). These particles were also strongly stained for H1.2 (Fig. 8C). Many of these particles lacked major chromatin moieties (Fig. 8, D–F). These particles exhibited size heterogeneity like the endogenous chromosome-embedded NORs, suggesting that NORs are structurally robust and remain intact during homogenization, which has, however, broken down the chromosomes (*e.g.* Fig. 8, G–I).
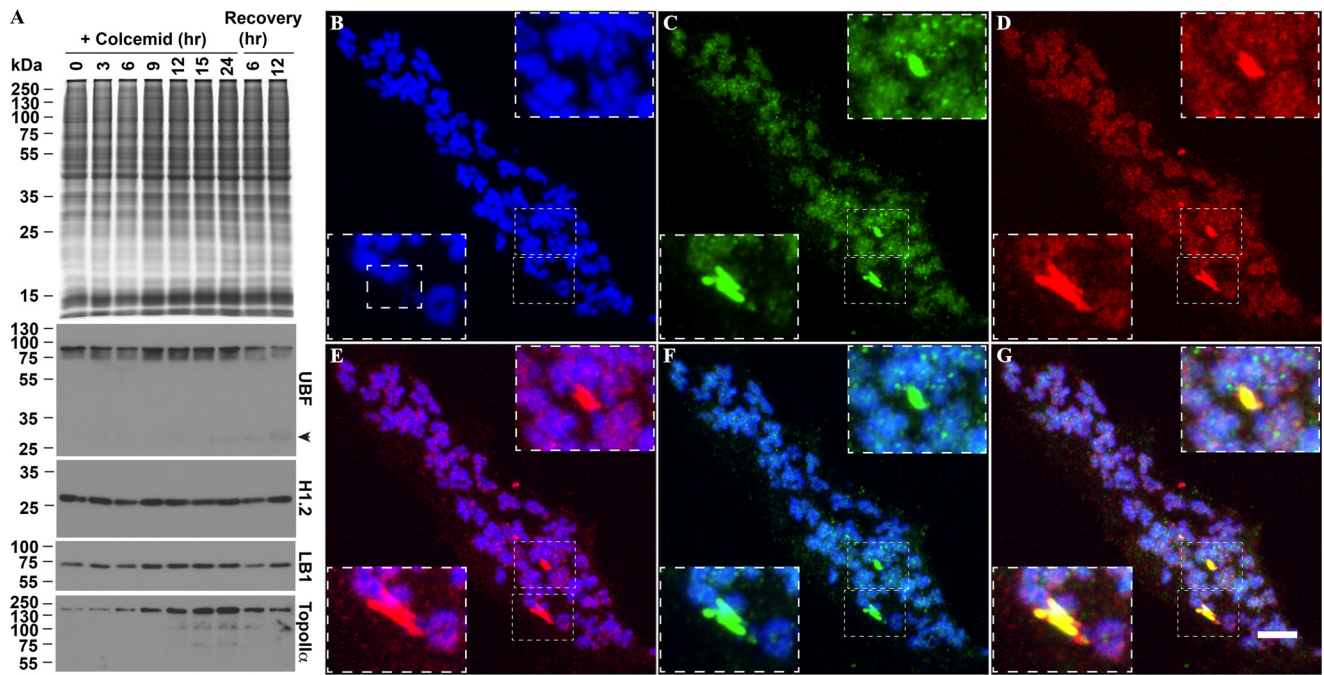
Figure 6. Sustained H1.2 expression during interphase and mitosis and the structural independence of NORs. *A*, HeLa cells were treated for up to 24 h with colcemid (0.1 μg/ml) and harvested at 3-h intervals to generate cell lysates. After 24 h, colcemid was removed. The cells were further cultured for 6 and 12 h. Sample loading was normalized based on total cellular proteins (*top panel*). UBF, H1.2, lamin B1, and TopoIIα levels were determined by Western blotting. *Arrowhead*, possible UBF fragment. *B–G*, HeLa cells treated with colcemid (0.1 μg/ml, 15 h) were homogenized. After centrifugation, chromosomes were harvested in the pellets. On coverslips, these chromosomes were fixed and stained with mouse anti-UBF (Cy3, *red*), rabbit anti-H1.2 (AF488, *green*), and DAPI (*blue*) and analyzed by confocal microscopy. 3D images were reconstructed from the 0.36-μm serial section images collected. *B–D*, single signals. *E–G*, merged signals. Two prominent NORs are highlighted by *squares* and presented at higher magnifications. *Scale bar*, 5 μm.

Conclusions

NORs are well known mitotic structures, but their structures and functions remain inadequately defined. NORs were known to form around rDNA loci during mitosis through UBF. Our data show that they are structurally independent of the chromosome bodies. The linker H1 histones were known as chromatin-binding proteins that facilitate chromatin compaction. Our data show that, among the H1 variants, H1.2 binds to UBF, and during mitosis, it is recruited to NORs like UBF. The results collectively suggest additional functions for NORs in addition to organizing the rDNA loci during mitosis and also show selective H1.2 association with this structure. However, the distribution of H1 variants, UBF, and other nuclear proteins is probably often determined by more than one binding partner.

Discussion

The nucleoli synthesize >50% of all cellular RNA in the form of pre-rRNA (1). Being embedded in the chromatin network, nucleoli can still afford dynamic molecular exchanges and morphological changes (13, 14). Nucleoli form around the rDNA loci, and as a master nucleolar organizer, UBF appears to bind persistently to these loci throughout the cell cycle (31, 32). Although the molecular scaffolds that shape the nucleoli and their mitotic remnants, *i.e.* NORs, remain limitedly understood, these inevitably involve the two core elements, *i.e.* rDNA and UBF. In this study, we used UBF-Sepharose to identify novel UBF-binding proteins from the nuclear extract (Fig. 1).

Identification of histone H1.2 as a UBF-binding protein was at first contradictory to a subsequent observation that these two proteins distributed disparately in the interphase nuclei. How-

ever, this paradox was reconciled at mitosis when the chromatins compact to form chromosomes, and the nucleoli mostly dispersed, leaving remnants near the rDNA loci to form NORs of different sizes. UBF was condensed in these NORs, and H1.2 followed UBF into NORs apparently in proportion with UBF. Both UBF and H1.2 were divided equivalently into daughter nuclei. After division, NORs expanded into nucleoli, and H1.2 exited the nucleolar regions demarcated by UBF. These observations illustrate a novel mechanism by which a non-nucleolar protein was selectively recruited into NORs during mitosis.

It is unclear how many other proteins may be similarly or differently recruited into NORs like H1.2, but among the six H1 variants examined (H1.1–H1.5 and H1.x), the other five were not found in NORs (Figs. S1 and S2). Although the H1.0 variant was reported to bind to numerous nucleolar proteins (44), it was not concentrated in interphase nucleoli or mitotic NORs (Fig. S2). Although the subcellular localization of H1.3 in HeLa cells was not clearly defined because of its low expression, the data overall stress a specific relationship among H1.2, UBF, and NORs.

When H1.2 was recruited to NORs, it also diminished in the compacted chromosomes (Fig. 3), giving the initial impression that the otherwise chromatin-associated H1.2 in interphase nuclei was depleted from the chromosomes and all transferred into NORs. However, H1.2 was actually present inside chromosomes, although it was masked from antibody detection. When isolated chromosomes were spread on glass coverslips, H1.2 became detectable in these chromosomes (Fig. 5). When endogenous chromosomes were digested with DNase, H1.2 also became detectable in the residual chromosomes (Fig. 7).
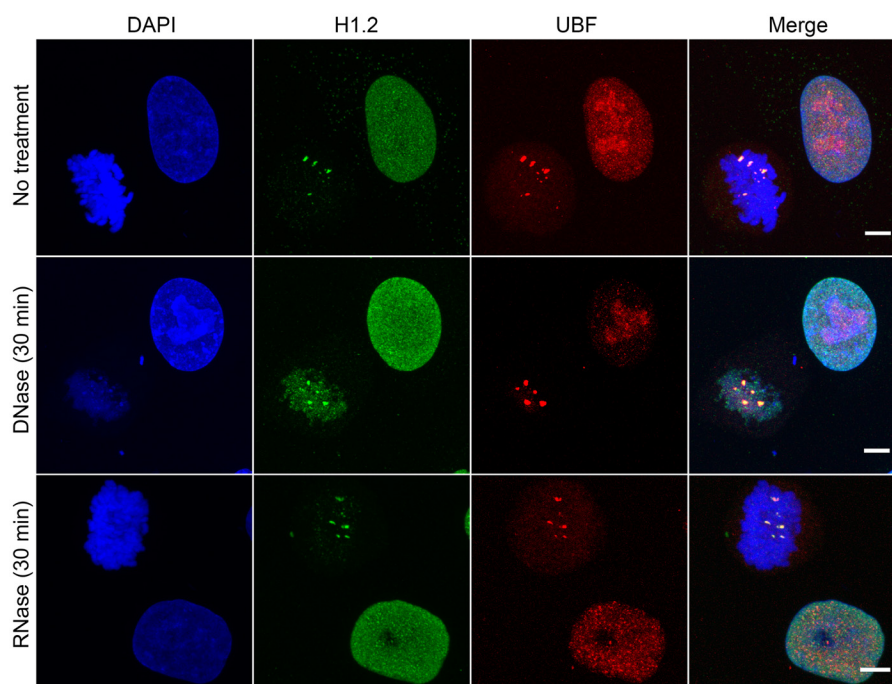
Figure 7. Revelation of chromosome-associated H1.2 after DNase digestion. HeLa cells on glass coverslips were fixed and permeabilized. *Top panels*, cells were incubated with the DNase buffer for 30 min before staining with rabbit anti-H1.2 and mouse anti-UBF antibodies. The cells were then stained using secondary goat anti-rabbit (AF488, *green*) and anti-mouse (Cy3, *red*) IgG. *Middle panels*, permeabilized cells were incubated with DNase for 30 min before immunostaining. *Bottom panels*, permeabilized cells were treated with RNase A for 30 min before immunostaining. Coverslips were mounted with a DAPI-containing medium, and serial 0.36-μm section images were captured by confocal microscopy. 3D images were reconstructed using the Imaris software. *Scale bars*, 5 μm.
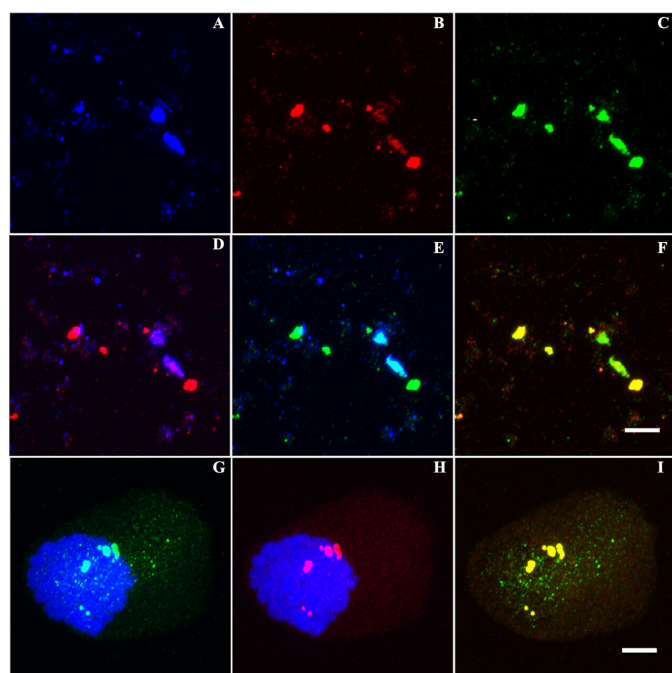

Figure 8. NORs are separable from chromosomes. *A–F*, HeLa cells were treated with colcemid for 15 h and homogenized at 10-μm clearance. After centrifugation, pelleted materials were adhered to coverslips and fixed. These were stained first with mouse anti-UBF and rabbit anti-H1.2 antibodies and then stained with secondary goat anti-mouse (Cy3, *red*) and anti-rabbit (AF488, *green*) IgG. After mounting with DAPI-counting medium, serial 0.36-μm section images were captured by confocal microscopy. 3D images were reconstructed using the Imaris software. *A–C*, single signals. *D–F*, merged signals. *G–I*, HeLa cells were treated for 15 h with colcemid on coverslips and then fixed and stained for UBF, H1.2, and the chromatins. Merged 3D images are shown: *G*, H1.2 and chromatins, *H*, UBF and chromatins, *I*, H1.2 and UBF. *Scale bars*, 5 μm.

Therefore, it appears that two pools of nuclear H1.2 exist with one binding to UBF and being recruited to NORs and the other binding to the chromatins and being compacted inside the chromosomes. H1.2 interaction with UBF appears to require its CTD, but this region is also required for H1.2 to interact with DNA and RNA (Fig. S1). The two pools of H1.2 could result from UBF competition with chromatin and other H1.2-binding partners for the H1.2 CTD. Some undefined post-translational modifications may also influence H1.2 interaction with UBF and the ultimate distribution of H1.2 and other H1 variants (38).

In interphase nuclei, UBF is abundant in the nucleoli, but it is also distributed among the nucleoplasmic chromatins (Fig. 3). UBF has indeed been reported to associate with selected genes in the nucleoplasm (31–35). As a chromatin-binding protein, the broad distribution of H1.2 in the nucleoplasm is natural. It was its mitotic recruitment into NORs that was not expected, although it also became logical considering its newly found affinity for UBF. It is unclear whether this H1.2–UBF interaction persists in interphase nuclei or whether it is only induced during mitosis. In any case, this interaction was also implied, albeit not validated, in ActD-induced NOR-like structures in interphase nuclei (Fig. 5).

This unusual property of histone H1.2 prompted us to ascertain the specificity of the anti-H1.2 antibody and examine its potential cross-reactivity with other antigens. We first used this antibody to screen 11 human cell lines, including HeLa cells. By Western blotting, the antibody only reacted with one protein that was equivalent to H1.2 in size (Fig. S2). We also screened the antibody against six purified H1 variants (H1.1–H1.5 and

H1.x), and it only reacted with H1.2 (Fig. S3). The possibility that the antibody cross-reacted with an epitope that was only induced during mitosis was also ruled out, because no additional proteins reacted with the antibody when metaphase cells were enriched in culture using colcemid (Fig. 6A). Finally, a 2-h ActD treatment was sufficient to induce NOR-like structures in interphase nuclei, and these structures were reacted by the anti-H1.2 antibody. Therefore, the antibody is specific for H1.2.

H1.2 is a non-nucleolar protein and has no known functions in rRNA biosynthesis or ribosome assembly. Its recruitment into mitotic NORs is also in contrast to most indigenous nucleolar proteins that instead exit these structures during mitosis. The implications of this phenomenon are unclear. H1.2 could be passenger molecules that are preserved in NORs during mitosis and are then faithfully transmitted to daughter cells without undergoing the usual dismantling experienced by most other nuclear proteins. During the 1970s through the 1990s, the search for nuclear scaffolds that could orient interphase nuclear chromatins identified H1 histone as an adaptor protein between the nuclear scaffolds and the chromatins (45). It is possible that the chromatin-associated and UBF-associated pools of H1.2 represent distinct nuclear scaffolds and are preserved in chromosomes and NORs, respectively, during mitosis for faithful transmission.

The rDNA loci lack classic nucleosomes and are instead organized into distinct conformations by dimeric UBF (46). They were also known as secondary constrictions in pioneer studies that led to modern investigations of the nucleolus (4, 7, 25, 47). These unique conformations may function to recruit and preserve certain nuclear configurations that cannot afford complete scrambling during mitosis. Alternatively, H1.2 may be required to form and maintain this conformation together with UBF and other unidentified and similarly recruited nuclear proteins.

Whether H1.2 indeed represents a preserved scaffold in NORs or whether it is required for NOR formation cannot be concluded based on current data. In mice, this is not expected to be essential to cell survival because H1.2$^{-/-}$ mice exhibit normal phenotype (48). However, inducible shRNA depletion of H1.2 in the human breast cancer cell line T47D caused cell cycle arrest (49). In the human fibrosacoma HT1080 cells, inducible shRNA depletion of UBF similarly caused complete growth arrest (32). Using the human HeLa cells, CRISPR-Cas9 knockdown of H1.2 led to no viable H1.2$^{-/-}$ clones (data not shown). If H1.2–UBF interaction and H1.2 recruitment to NORs are essential to cell survival, this is probably not compensated by other human H1 variants, although this is inconclusive for the most H1.2-related H1.3, which appears to bind to UBF but poorly expressed in HeLa cells.

In addition to H1.2 recruitment to NORs, H1.0, H1t, and H1.x have been reported to associate with nucleoli in different other contexts. As previously reported and also observed by us, H1.x was concentrated in interphase nucleoli, but it dispersed at mitosis like fibrillarin (Fig. 4 and Fig. S2) (39). H1t is a testis-specific H1 variant that is also expressed in different cancer cell lines (50). Like H1.x, H1t is also concentrated in interphase nucleoli, but it dispersed at mitosis. H1t concentration to nucleoli is likely to involve its binding to the rDNA repeats (50),

but this is unclear for H1.x. Using immobilized histone H1.0, Kalashnikova *et al.* (44) pulled down numerous ribosomal and other proteins from the nucleolar extract. However, these interactions have apparently not enriched H1.0 to the nucleoli or NORs (Fig. S2). H1.2 remains the only H1 variant that is known to be recruited to NORs.

Overall, our results demonstrated structural independence of NORs and H1.2 as a novel component of this structure. The different H1 variants exhibit dynamic subcellular distribution, which suggests distinct functional mechanisms. Although it appears that some H1 variants associate with the nucleoli or nucleolar elements, H1.2 is distinct in that it localizes in NORs. The ultimate subcellular localization of each H1 variant is likely to be determined by the multiple binding partners that interact with different regions on these versatile molecules.

Experimental procedures

Cell culture and reagents

Human cervical adenocarcinoma HeLa cells were cultured in DMEM containing 10% (v/v) HyClone fetal bovine serum, 100 units/ml penicillin, 100 μg/ml streptomycin, 2 mM L-glutamine at 37 °C and 5% CO_2. Colcemid (D1925) and a mouse anti-NPM1 antibody (B0556) were purchased from Sigma–Aldrich. Rabbit antibodies for histone H1.2 (ab17677), lamin B1 (LB1, ab16048), nucleolin (ab22758), fibrillarin (ab5821), centromere protein A (ab13939), and heterochromatin protein 1γ (HP1γ, ab10480) were obtained from Abcam (Cambridge, UK). Mouse antibodies for UBF (F9), lamin A/C (636), and TopoIIα (3F6) were obtained from Santa Cruz Biotechnology, Inc. Mouse anti-Pol II (CTD4H8) was obtained from Merck Millipore.

Nuclear extract

The nuclei were isolated from HeLa cells as previously described (17). Briefly, HeLa cells (2×10^8) were resuspended in 4 ml of a 0.25 M sucrose buffer (0.25 mM sucrose, 5.0 mM $MgCl_2$, and 10 mM Tris, pH 7.4) and, after homogenization at 10-μm clearance using the Isobiotec cell homogenizer (Isobiotec Precision Engineering, Heidelberg, Germany), centrifuged for 10 min at $600 \times g$. The nuclei were resuspended in 5 ml of a 2.2 M sucrose buffer (2.2 M sucrose, 5.0 mM $MgCl_2$, and 10 mM Tris, pH 7.4) and centrifuged for 30 min at $50,000 \times g$. The nuclei were then washed in the 0.25 M sucrose buffer and incubated for 1 h on ice in the same buffer containing 1% (v/v) Triton X-100 (4 ml). A mixture of protease inhibitors was included in these steps (Sigma-Aldrich). The lipid-depleted nuclei, named TxN, were washed and resuspended in the 0.25 M sucrose buffer (0.9 ml), before 0.1 ml of 5 M NaCl was added and vigorously mixed by pipetting. The nuclei swelled into a single colloidal gel to which 0.5 ml of the 0.25 M sucrose buffer containing 500 mM NaCl was added. After centrifugation for 10 min at $2,000 \times g$, the supernatant was collected. To the pellet, 0.5 ml of the 0.25 M sucrose buffer was added and vigorously mixed by pipetting. After centrifugation, supernatant was again collected. This step was repeated once, and all three supernatants were combined as a lipid/chromatin-free nuclear extract, known as TxNE. Its A_{280} reading is normally 1.0–2.0.

TxN were also adhered to coverslips by incubation for 5 min on ice and then incubated for 15 min on ice with the 0.25 M

sucrose buffer containing 100–500 mM NaCl. After fixation, these were immunostained for NPM1 and LB1 and analyzed by confocal microscopy.

Generation of affinity resins

cDNA for human UBF and histone H1.2 were PCR-amplified from HeLa cell RNA using the following primers: UBF (forward primer, 5′-CGGCTAGCATGAACGGAGAAGCCGACT-3′; reverse primer, 5′GCAAGCTTTCAGTTGGAGTCAGAGT-CTGA-3′) and histone H1.2 (forward primer, 5′-ATGGC-TAGCATGTCCGAGACTGCTCCTGCC-3′; reverse primer, 5′-TTCGGATCCGGGTTTTAGAAGTAGGCGTTCGC-3′). The cDNA fragments were cloned into the pET28 vector between NheI/HindIII (UBF) or NheI/BamHI (H1.2), and the vectors were expressed in *Escherichia coli* BL-21. The pET28 expression vectors for three H1.2 mutants were synthesized by Genescript (Piscataway, NJ) with flanking 5′ NdeI and 3′BamHI restriction sites: H1.2ΔNTD (5′-*GCTAGC*TCTG-GTCCCCCGGTGTCAGA……CGGCGCCCAAGAAGAAA <u>TAG</u>*GGATCC*-3′, amino acid 36–213), H1.2ΔCTD (5′-*GCT-AGC*ATGTCCGAGACTGCTCCTGC……CCTTTAAA-CTCAACAAG<u>TAG</u>*GGATCC*-3′, amino acid 1–109), and H1.2GD (5′-*GCTAGC*TCTGGTCCCCCGGTGTCAGA…… CCTTTAAACTCAACAAG<u>TAG</u>*GGATCC*-3′, amino acid 36–109). Restriction sites are in italics, and stop codons are underlined.

To purify these recombinant proteins, overnight bacteria cultures (5 ml) were diluted in 50 ml of L-broth containing kanamycin (30 µg/ml), and when A_{600} reading reached 0.6–0.8, isopropyl β-D-thiogalactopyranoside was added to 1 mM and further cultured for 3 h. Bacteria were harvested and sonicated in the binding buffer (50 mM sodium phosphate, 350 mM NaCl, and 10 mM imidazole, pH 7.4), and the supernatant was incubated overnight in a Poly-prep column (Bio-Rad) with 0.5 ml of nickel-nitrilotriacetic acid-agarose (Thermo Fisher Scientific). The columns were washed with 30 ml of binding buffer containing 20 mM imidazole and eluted at 150 mM imidazole.

Affinity chromatography

Purified UBF and H1.2 were coupled to CNBr-activated Sepharose 4B (GE Healthcare) to generate UBF- and H1.2-Sepharose. The resins were also derived with 1 M Tris (pH 8.0) (Tris-Sepharose) to use as a control. TxNE, which contained ~300 mM NaCl, was diluted 2-fold in the 0.25 M sucrose buffer (2 ml) and, in a Poly-prep column, incubated with 0.5 ml of UBF-, H1.2-, or Tris-Sepharose for 2 h at 4 °C. The flowthrough fractions were collected, and the columns were each washed with 20 ml of a washing butter (50 mM Tris, pH 7.4, and 150 mM NaCl). The columns were eluted at 500 mM NaCl (50 mM Tris, pH 7.4, and 500 mM NaCl) in 150-µl fractions. Similarly, purified H1.2 was applied to UBF-Sepharose and purified UBF was applied to H1.2-Sepharose.

Affinity pulldown of H1 variants and H1.2 mutant proteins

H1 variants were generated as detailed in Fig. S3. Three H1.2 mutants were generated by deleting its NTD (H1.2ΔNTD), CTD (H1.2ΔCTD), or both NTD and CTD (H1.2GD). 200 µl of each purified H1 protein or H1.2 mutant (100–200 µg/ml) was

incubated with 50 µl of UBF-Sepharose for 2 h. As a control, H1.2 was also incubated with Tris-Sepharose. The supernatants were reserved, and the resins were each washed three times in the washing buffer. Bound proteins were eluted using 100 µl of 1 M NaCl in the washing buffer. The input, supernatant, and elution from each experiment were analyzed by SDS-PAGE and Coomassie Blue staining.

SDS-PAGE and Western blotting

Samples separated on 12.5 or 18% (w/v) SDS-PAGE gels were either stained with Coomassie Blue or electrotransferred for Western blotting. The blots were blocked for 1 h in TBS-T (50 mM Tris, 150 mM NaCl, pH 7.4, and 0.1% (v/v) Tween 20) containing 5% (w/v) nonfat milk and then incubated overnight at 4 °C with different primary antibodies (0.5 µg/ml). After washing in TBS-T, the blots were incubated for 2 h with horseradish peroxidase–conjugated goat anti-mouse or anti-rabbit IgG. Signals were visualized using the Pierce Supersignal West Pico Chemiluminescent substrate (Thermo Fisher Scientific). Some blots were stripped for 30 min at 50 °C in 62.5 mM Tris (pH 6.8) containing 0.1 M 2-mecaptoethanol and 2% (w/v) SDS and then reprobed with a different antibody.

LC-MS/MS

Proteins eluted from UBF-Sepharose were heated for 10 min at 100 °C in the presence of dithiothreitol (10 mM) without dye and then alkylated for 30 min at room temperature with iodoacetamide (20 mM) in the dark. The samples were separated on 12.5% (w/v) gels and stained with Coomassie Blue. Selected bands were excised and, after trypsin digestion, extracted and analyzed by liquid chromatography–tandem mass spectrometry (Experimental Therapeutics Centre, Biopolis Shared Facilities, A-Star, Singapore). The data were analyzed and presented using the Scaffold_4.0.5 software (Proteome Software, Inc., Portland, OR).

Generation of metaphase cells and isolation of chromosomes

HeLa cells (80% confluency) were treated with colcemid (0.1 µg/ml) for up to 24 h. The cells were harvested at 3-h intervals in SDS-PAGE sample buffer. After 24 h, the cells were also washed to remove colcemid and further cultured for 6 or 12 h. By Western blotting, H1.2, UBF, TopoIIα, and LB1 were detected in these cell lysates.

To isolate chromosomes, HeLa cells ($\sim 1 \times 10^8$) were treated for 15 h with colcemid, and the detached metaphase cells were washed and resuspended in the 0.25 M sucrose buffer (2 ml). The cells were homogenized at 18-µm clearance, and after centrifugation for 10 min at 600 × g, the pelleted chromosomes were resuspended in the 0.25 M sucrose buffer. To break down the chromosomes, metaphase cells were homogenized at 10-µm clearance. The chromosome fragments were adhered on coverslips by incubation for 10 min on ice and after fixation were immunostained using mouse anti-UBF and rabbit anti-H1.2 antibodies.

Confocal microscopy

HeLa cells cultured on coverslips were fixed for 30 min in 1% (w/v) paraformyldehyde and then permeabilized for 1 h in PBS

containing 1% (v/v) Triton X-100. The cells were incubated for 1 h with mouse anti-UBF and a rabbit antibody for histone H1.2, nucleolin, or fibrillarin. The cells were also stained with antibodies for H1.0, H1.1, H1.3, H1.4, H1.5, and H1.x (Fig. S2). After washing, the cells were incubated with goat anti-mouse (Cy3) and anti-rabbit (Alexa Fluor 488 or AF488) IgG. The permeabilized cells were also incubated for 30 min at room temperature with either DNase from the NucleoSpin RNA isolation kit (Machery–Nagel, Duren, Germany) or RNase A at 1 mg/ml in the 0.25 mM sucrose buffer (Qiagen) before immunostaining. HeLa cells were also treated for 2 h with ActD (40 ng/ml) to block Pol I transcription (40, 41). These cells were similarly fixed, permeabilized, and immunostained with a mouse anti-UBF antibody and a rabbit antibody for H1.2 or nucleolin. The cells were washed and mounted using the VectorShield medium containing 4′,6′-diamino-2-phenylindole. and analyzed using a FluoView FV1000 confocal microscope equipped with a $100\times$ oil objective (aperture 1.45) and Cool/SNAP HQ2 image acquisition camera (Olympus). Images were acquired with the FV-ASW 1.6b software and analyzed using the Imaris software (Bitplane AG). With TxN, isolated chromosomes, and chromosome fragments, these were first adhered to coverslips by incubation for 10 min on ice and, after fixation, similarly immunostained and analyzed by confocal microscopy.

Scanning electron microscopy

TxN were adhered to coverslips by incubation for 10 min on ice. After fixing for 2 h in 2.5% (w/v) glutaraldehyde, the nuclei were washed in PBS and oxidized for 30 min in 1% (w/v) OsO_4 (pH 7.4). After washing, the coverslips were dehydrated using increasing concentrations of ethanol (*i.e.* 50, 75, 95, and 100%). The coverslips were then equilibrated and dried in liquid CO_2 using the EM CPD 030 Critical Point Dryer (Leica Camera AG, Wetzlar, Germany) and gold-coated for 100 s at 30 mA using a BAL-TEC SCD 005 Sputter Coater (Leica). The samples were analyzed at 10 KV and 20 μA emission current, using the JSM-6701F field emission scanning microscope (JOEL Ltd., Tokyo, Japan).

References

1. Shaw, P. J., and Jordan, E. G. (1995) The nucleolus. *Annu. Rev. Cell Dev. Biol.* **11,** 93–121 CrossRef Medline
2. Olson, M. O., Hingorani, K., and Szebeni, A. (2002) Conventional and nonconventional roles of the nucleolus. *Int. Rev. Cytol* **219,** 199–266 CrossRef Medline
3. Pederson, T. (2011) The nucleolus. *Cold Spring Harb. Perspect. Biol.* **3,** a000638 Medline
4. McClintock, B. (1934) The relation of a particular chromosomal element to the development of the nucleoli in *Zea mays. Z. Zellforsch.* **21,** 33
5. Henderson, A. S., Warburton, D., and Atwood, K. C. (1972) Location of ribosomal DNA in the human chromosome complement. *Proc. Natl. Acad. Sci. U.S.A.* **69,** 3394–3398 CrossRef Medline
6. Farley, K. I., Surovtseva, Y., Merkel, J., and Baserga, S. J. (2015) Determinants of mammalian nucleolar architecture. *Chromosoma* **124,** 323–331 CrossRef Medline
7. McStay, B. (2016) Nucleolar organizer regions: genomic "dark matter" requiring illumination. *Genes Dev.* **30,** 1598–1610 CrossRef Medline
8. Scheer, U., and Weisenberger, D. (1994) The nucleolus. *Curr. Opin Cell Biol.* **6,** 354–359 CrossRef Medline
9. Sirri, V., Hernandez-Verdun, D., and Roussel, P. (2002) Cyclin-dependent kinases govern formation and maintenance of the nucleolus. *J. Cell Biol.* **156,** 969–981 CrossRef Medline
10. Raska, I., Shaw, P. J., and Cmarko, D. (2006) Structure and function of the nucleolus in the spotlight. *Curr. Opin. Cell Biol.* **18,** 325–334 CrossRef Medline
11. Németh, A., and Längst, G. (2011) Genome organization in and around the nucleolus. *Trends Genet.* **27,** 149–156 CrossRef Medline
12. Cai, Y., Wee, S. Y. K., Chen, J., Teo, B. H. D., Ng, Y. L. C., Leong, K. P., and Lu, J. (2017) Broad susceptibility of nucleolar proteins and autoantigens to complement C1 protease degradation. *J. Immunol.* **199,** 3981–3990 CrossRef Medline
13. Phair, R. D., and Misteli, T. (2000) High mobility of proteins in the mammalian cell nucleus. *Nature* **404,** 604–609 CrossRef Medline
14. Brangwynne, C. P., Mitchison, T. J., and Hyman, A. A. (2011) Active liquid-like behavior of nucleoli determines their size and shape in *Xenopus laevis* oocytes. *Proc. Natl. Acad. Sci. U.S.A.* **108,** 4334–4339 CrossRef Medline
15. Larson, A. G., Elnatan, D., Keenen, M. M., Trnka, M. J., Johnston, J. B., Burlingame, A. L., Agard, D. A., Redding, S., and Narlikar, G. J. (2017) Liquid droplet formation by HP1α suggests a role for phase separation in heterochromatin. *Nature* **547,** 236–240 CrossRef Medline
16. Desjardins, R., Smetana, K., Steele, W. J., and Busch, H. (1963) Isolation of nucleoli of the Walker carcinosarcoma and liver of the rat following nuclear disruption in a French pressure cell. *Cancer Res.* **23,** 1819–1823 Medline
17. Cai, Y., Teo, B. H., Yeo, J. G., and Lu, J. (2015) C1q protein binds to the apoptotic nucleolus and causes C1 protease degradation of nucleolar proteins. *J. Biol. Chem.* **290,** 22570–22580 CrossRef Medline
18. Cheutin, T., O'Donohue, M. F., Beorchia, A., Vandelaer, M., Kaplan, H., Deféver, B., Ploton, D., and Thiry, M. (2002) Three-dimensional organization of active rRNA genes within the nucleolus. *J. Cell Sci.* **115,** 3297–3307 Medline
19. Koberna, K., Malínský, J., Pliss, A., Masata, M., Vecerova, J., Fialová, M., Bednár, J., and Raska, I. (2002) Ribosomal genes in focus: new transcripts label the dense fibrillar components and form clusters indicative of "Christmas trees" *in situ. J. Cell Biol.* **157,** 743–748 CrossRef Medline
20. Miller, O. L., Jr., and Beatty, B. R. (1969) Visualization of nucleolar genes. *Science* **164,** 955–957 CrossRef Medline
21. Mougey, E. B., O'Reilly, M., Osheim, Y., Miller, O. L., Jr., Beyer, A., and Sollner-Webb, B. (1993) The terminal balls characteristic of eukaryotic rRNA transcription units in chromatin spreads are rRNA processing complexes. *Genes Dev.* **7,** 1609–1619 CrossRef Medline
22. Savino, T. M., Gébrane-Younès, J., De Mey, J., Sibarita, J. B., and Hernandez-Verdun, D. (2001) Nucleolar assembly of the rRNA processing machinery in living cells. *J. Cell Biol.* **153,** 1097–1110 CrossRef Medline
23. Roussel, P., André, C., Comai, L., and Hernandez-Verdun, D. (1996) The rDNA transcription machinery is assembled during mitosis in active NORs and absent in inactive NORs. *J. Cell Biol.* **133,** 235–246 CrossRef Medline
24. Heix, J., Vente, A., Voit, R., Budde, A., Michaelidis, T. M., and Grummt, I. (1998) Mitotic silencing of human rRNA synthesis: inactivation of the promoter selectivity factor SL1 by cdc2/cyclin B-mediated phosphorylation. *EMBO J.* **17,** 7373–7381 CrossRef Medline

25. Ghosh, S., and Paweletz, N. (1990) The nucleolar chromatin and the secondary constriction. *Cell Biol. Int. Rep.* **14,** 681–687 CrossRef Medline

26. Gébrane-Younès, J., Fomproix, N., and Hernandez-Verdun, D. (1997) When rDNA transcription is arrested during mitosis, UBF is still associated with non-condensed rDNA. *J. Cell Sci.* **110,** 2429–2440 Medline

27. Goodpasture, C., and Bloom, S. E. (1975) Visualization of nucleolar organizer regions im mammalian chromosomes using silver staining. *Chromosoma* **53,** 37–50 CrossRef Medline

28. Russell, J., and Zomerdijk, J. C. (2005) RNA-polymerase-I-directed rDNA transcription, life and works. *Trends Biochem. Sci.* **30,** 87–96 CrossRef Medline

29. Roussel, P., Andre, C., Masson, C., Geraud, G., and Hernandez-Verdun, D. (1993) Localization of the RNA polymerase I transcription factor hUBF during the cell cycle. *J. Cell Sci.* **104,** 327–337

30. O'Sullivan, A. C., Sullivan, G. J., and McStay, B. (2002) UBF binding *in vivo* is not restricted to regulatory sequences within the vertebrate ribosomal DNA repeat. *Mol. Cell. Biol.* **22,** 657–668 CrossRef Medline

31. Mais, C., Wright, J. E., Prieto, J. L., Raggett, S. L., and McStay, B. (2005) UBF-binding site arrays form pseudo-NORs and sequester the RNA polymerase I transcription machinery. *Genes Dev.* **19,** 50–64 CrossRef Medline

32. Grob, A., Colleran, C., and McStay, B. (2014) Construction of synthetic nucleoli in human cells reveals how a major functional nuclear domain is formed and propagated through cell division. *Genes Dev.* **28,** 220–230 CrossRef Medline

33. Zentner, G. E., Saiakhova, A., Manaenkov, P., Adams, M. D., and Scacheri, P. C. (2011) Integrative genomic analysis of human ribosomal DNA. *Nucleic Acids Res.* **39,** 4949–4960 CrossRef Medline

34. Sanij, E., Diesch, J., Lesmana, A., Poortinga, G., Hein, N., Lidgerwood, G., Cameron, D. P., Ellul, J., Goodall, G. J., Wong, L. H., Dhillon, A. S., Hamdane, N., Rothblum, L. I., Pearson, R. B., Haviv, I., *et al.* (2015) A novel role for the Pol I transcription factor UBTF in maintaining genome stability through the regulation of highly transcribed Pol II genes. *Genome Res.* **25,** 201–212 CrossRef Medline

35. Grueneberg, D. A., Pablo, L., Hu, K. Q., August, P., Weng, Z., and Papkoff, J. (2003) A functional screen in human cells identifies UBF2 as an RNA polymerase II transcription factor that enhances the β-catenin signaling pathway. *Mol. Cell. Biol.* **23,** 3936–3950 CrossRef Medline

36. Malarkey, C. S., and Churchill, M. E. (2012) The high mobility group box: the ultimate utility player of a cell. *Trends Biochem. Sci.* **37,** 553–562 CrossRef Medline

37. Izzo, A., and Schneider, R. (2016) The role of linker histone H1 modifications in the regulation of gene expression and chromatin dynamics. *Biochim. Biophys. Acta* **1859,** 486–495 CrossRef Medline

38. Fyodorov, D. V., Zhou, B. R., Skoultchi, A. I., and Bai, Y. (2017) Emerging roles of linker histones in regulating chromatin structure and function. *Nat. Rev. Mol. Cell Biol.*

39. Takata, H., Matsunaga, S., Morimoto, A., Ono-Maniwa, R., Uchiyama, S., and Fukui, K. (2007) H1.X with different properties from other linker histones is required for mitotic progression. *FEBS Lett.* **581,** 3783–3788 CrossRef Medline

40. Jordan, E. G., and McGovern, J. H. (1981) The quantitative relationship of the fibrillar centres and other nucleolar components to changes in growth conditions, serum deprivation and low doses of actinomycin D in cultured diploid human fibroblasts (strain MRC-5). *J. Cell Sci.* **52,** 373–389 Medline

41. Yung, B. Y., Bor, A. M., and Chan, P. K. (1990) Short exposure to actinomycin D induces "reversible" translocation of protein B23 as well as "reversible" inhibition of cell growth and RNA synthesis in HeLa cells. *Cancer Res.* **50,** 5987–5991 Medline

42. Zhou, B.R., Feng, H., Kato, H., Dai, L., Yang, Y., Zhou, Y., and Bai, Y. (2013) Structural insights into the histone H1-nucleosome complex. *Proc. Natl. Acad. Sci. U.S.A.* **110,** 19390–19395 CrossRef Medline

43. Maeshima, K., and Laemmli, U. K. (2003) A two-step scaffolding model for mitotic chromosome assembly. *Dev. Cell* **4,** 467–480 CrossRef Medline

44. Kalashnikova, A. A., Winkler, D. D., McBryant, S. J., Henderson, R. K., Herman, J. A., DeLuca, J. G., Luger, K., Prenni, J. E., and Hansen, J. C. (2013) Linker histone H1.0 interacts with an extensive network of proteins found in the nucleolus. *Nucleic Acids Res.* **41,** 4026–4035 CrossRef Medline

45. Izaurralde, E., Käs, E., and Laemmli, U. K. (1989) Highly preferential nucleation of histone H1 assembly on scaffold-associated regions. *J. Mol. Biol.* **210,** 573–585 CrossRef Medline

46. Stefanovsky, V. Y., Pelletier, G., Bazett-Jones, D. P., Crane-Robinson, C., and Moss, T. (2001) DNA looping in the RNA polymerase I enhancesome is the result of non-cooperative in-phase bending by two UBF molecules. *Nucleic Acids Res.* **29,** 3241–3247 CrossRef Medline

47. Heitz, E. (1931) Die ursache der gesetzmassigen zahl, lage, form und grosse pflanzlicher nukleolen. (The cause of number, position, form and size of plant nucleoli.) *Planta* **12,** 69

48. Fan, Y., Sirotkin, A., Russell, R. G., Ayala, J., and Skoultchi, A. I. (2001) Individual somatic H1 subtypes are dispensable for mouse development even in mice lacking the H1(0) replacement subtype. *Mol. Cell. Biol.* **21,** 7933–7943 CrossRef Medline

49. Sancho, M., Diani, E., Beato, M., and Jordan, A. (2008) Depletion of human histone H1 variants uncovers specific roles in gene expression and cell growth. *PLoS Genet.* **4,** e1000227 CrossRef Medline

50. Tani, R., Hayakawa, K., Tanaka, S., and Shiota, K. (2016) Linker histone variant H1T targets rDNA repeats. *Epigenetics* **11,** 288–302 CrossRef Medline

ASBMB

J. Biol. Chem. (2018) 293(7) 2358–2369 **2369**